DOE/BC/14899-25
Distribution Category UC-122

Visualization and Simulation of Immiscible Displacement in Fractured Systems Using Micromodels: Steam Injection

By
Yanis C. Yortsos

July 1995

Work Performed Under Contract No. DE-FG22-93BC14899

Prepared for
U.S. Department of Energy
Assistant Secretary for Fossil Energy

Thomas B. Reid, Project Manager
Bartlesville Project Office
P.O. Box 1398
Bartlesville, OK 74005

Prepared by
University of Southern California
Petroleum Engineering Program
Department of Chemical Engineering
Los Angeles, CA 90089-1211

DISCLAIMER

Contents

List of Figures

ABSTRACT

A study of steam and hot water injection processes in micromodel geometries that mimic a matrix-fracture system was undertaken. The followings were observed:

Light components existing in the crude oil generated a very high efficient gas-drive at elevated temperatures. This gas generation in conjunction with natural surfactant existing in the crude oil, lead to the formation of a foam in the fracture and to improved displacement in the matrix. We observed that the steam enters the fracture and the matrix depending on whether the steam rate exceeds or not the critical values. The resulting condensed water also moves preferentially into the matrix or the fracture depending on the corresponding capillary number. Since steam is a non-wetting phase as a vapor, but becomes a wetting phase when condensed in a water-wet system, steam injection involves both drainage and imbibition. It was found that all of the oil trapped by the condensed water can be mobilized and recovered when in contact with steam.

We also examined hot-water displacement. In comparison with cold-water experiments at the same capillary number, a higher sweep efficiency for both light and heavy oils was observed. It was found that the foam generated in the fracture during hot-water injection, is more stable than in steamflooding. Nonetheless, hot-water injection resulted into less efficient displacement in its absence.

1 INTRODUCTION

Steam injection is a potentially effective method for the recovery of heavy oil from reservoirs. There are large accumulations of heavy crude and tar sands recoverable by steam injection in certain parts of the world, especially in Western Canada, Central Venezuela and in California and Utah in the U.S. [20]. Steam injection can also be used to recover light crude, at least as or even more effectively than waterflooding [20]. Naturally fractured reservoir may contain 25-30% of the world supply of oil [23]. Thus, steam injection in fractured reservoirs has a high potential importance in oil production.

Unfortunately, the understanding of steam injection in fractured systems is currently based mostly on phenomenology and typically consists of applying a double porosity formalism to commercial steam simulators [5], [11], [13]. Most of these use capillary imbibition as the key mechanism for the exchange of fluids between the matrix blocks and the fracture network. Such a purely numerical approach offers little to further our insight in the process. As a reasonable alternative, the study of injection (both experimental and numerical) in model geometries that mimic fractured systems was considered. Good candidates are Hele-Shaw cells and glass micromodels. Such special geometries are considered in this research.

1.1 Steamflooding in Fractured Systems

Sahuquet and Ferrier [22] carried out a steam-drive pilot in a fractured, carbonated reservoir. They observed increased oil production without early heat or steam breakthrough. They also reported CO_2 generation, which is the result of dissociation of steam with carbonated rocks, which improved the process efficiency.

Dreher et al. [8] carried out some laboratory experiments and reservoir simulation for hot water and steam-flooding in carbonate, fractured rocks. They observed very high oil recovery from the matrix when either hot water or steam was injected into the fractures. CO_2 generation, oil swelling and viscosity reduction were mentioned as enhanced oil recovery mechanisms.

Jensen [11] performed waterflooding and steam injection on sandstone and carbonate fractured cores. He found imbibition as the most important recovery mechanism in fractured sandstone, while thermal swelling and viscosity reduction were the major recovery mechanisms in fracture carbonate cores. He also found changes in the endpoint saturation in fractured sandstones, which

tend to the lower final oil saturation (higher oil recovery) in solid cores compared to fractured cores and to increase the oil recovery for horizontal and narrow fractures compared to vertical and larger fracture widths respectively.

van Wunnik and Kit [25] presented an analytical solution for steam injection into a fractured reservoir in which gravity drainage is the main mechanism of the oil production. They first gave an evaluation of the mixing rate and the steam/gas mixing zone in fracture networks. Using the temperature distribution in the reservoir and overburden rock, they derived the oil production rate by the mechanisms of gravity drainage and oil expansion.

Chen et al. [5] developed a dual porosity model for the simulation of thermal effects in naturally fractured reservoirs. Their simulator was 3-D, three-phase, and compositional. Matrix blocks were sub-divided into 2-D grids in order to consider effects of gravity, capillary pressure, and mass and energy transfer between fractures and matrix blocks.

Finally, Lee and Tan [13] introduced a multi-porosity/multi-permeability thermal simulator. They presented an iterative solution technique to create connection between any pair of blocks.

Boberg [1] discussed various mechanisms involved during the steamflooding of homogeneous reservoirs. A combination of mobility ratio improvement at the elevated temperature of the steam and a condensing gas drive displacement by the steam itself were mentioned as primarily mechanisms. Cracking of the oil at elevated temperatures, thermal expansion of the oil, solvent extraction, and temperature effects on the relative permeability to oil and water in the water zone ahead of the steam front are other mechanisms in steamflooding. He attributed the reason to a very low residual oil saturation after steamflooding in that hundreds of pore volumes of steam vapor travel through steam zone to the condensation front.

Willman et al. [26] examined the importance of the distillation of the light hydrocarbons during steamflooding in non-fractured cores. For a 50% distillable oil, they found up to 19.5 percent additional recovery due to distillation. The displacement efficiency of steam was also compared with that of hot and cold water. For the crude oil under investigation, the recovery for steamflooding was over 90% while under hot-waterfloods and cold-waterfloods they were around 70% and 60%, respectively.

Unlike homogeneous reservoirs, the injected steam does not sweep the porous media in fractured systems but preferentially flow through high conductivity fractures. Therefore, the above recovery

mechanisms act differently in fractured systems. Reis [21] reviewed oil recovery mechanisms in fractured reservoirs during steam injection. Thermal expansion and gas generation were described as two key mechanisms at high temperatures. He also described several other mechanisms as follows:

Thermal Expansion: Fluid and rock minerals expand by increasing temperature. Since the expansion of matrix minerals reduces the porosity, a differential thermal expansion of the order of 0.05%/°F is created by the combination of porosity reduction and fluid expansion. These effects result in the expulsion of fluids from the matrix into the fracture. In addition, the mechanism of heating in fractured reservoirs is mostly by conduction, while in a homogeneous system heat is transferred mainly by convection through the condensation of steam.

Capillary Imbibition: For water-wet reservoirs, capillary imbibition forces water in the fracture network into the matrix block through the smallest pores. Capillary imbibition, which depends on the brine/oil/rock system, may increase or decrease with temperature depending on the oil composition.

Gravity Drainage: Gas and water also transfer from fractures into surrounding matrix by gravity forces. The differential hydrostatic head between water in the fracture and a 35° API oil is only 0.065 psi/ft, while it is of the order of 0.3 psi/ft for gas in the fracture. Therefore, gravity drainage will have high potential recovery mechanism in gas filled fractures and thick formations.

Gas Generation: During steam injection, CO_2 generation was observed [22]. Light hydrocarbon components can also be generated during steam injection. As the temperature of reservoir increases, the volume of the generated gas also increases and displaces oil from the matrix towards the fracture. The distillation of light components at steam temperature is not significant in fractured system because the matrix blocks are not swept by the steam.

Solution Gas-Drive: Solution gas-drive can occur if the two phase envelope of a crude oil intersect the saturated steam curve. Reis [21] mentioned that in reservoir containing an initial gas saturation, this gas would expand upon heating and behave similar to a reservoir with an active solution gas-drive.

Some other mechanisms were also discussed by Reis [21], including chemical alteration of oil, cyclic pressure depletion, in-situ steam generation, alteration of the rock matrix, oil generation and rock compaction.

1.2 Flow Visualization Techniques

Flow visualization is a valuable device that enables us to understand some of the complex pore level mechanisms of multiphase flow in porous media, can confirm theories and upgrade computer simulation. Substantial efforts have been undertaken not only to visualize fluid flow during immiscible displacements [17, 18], but also for solution gas-drive [6], gravity drainage [27], and EOR processes, such as foam flow [4], surfactant and polymer flooding [7]. Although observing fluid flow in a single capillary tube or doublets is very useful, especially for the study of wetting phenomena [2], these tools are too simple to mimic the complex structure of capillary channels in real porous media. Therefore, investigators have been continuously searching for models with closer similarity to porous media. Typically, they make use of transparent Hele-Shaw cells, glass bead packs or micromodels. Persoff et al. [19] used 2 transparent rough-walled surfaces to simulate a single fracture. The history of the fabrication of etched glass and resin micromodels has been reviewed by Buckley [3]. In spite of the fact that such micromodels are restricted to two dimensions, they have been very useful in understanding the complex relationship between the geometry and topology of the medium and the solid/fluid interactions [9, 14, 15, 16]. Recently, Hornbrook et al. [10] developed a new procedure to construct a high resolution replica of a porous medium. They transferred a digital image of a thin section onto a silicon wafer. The silicon wafer can be oxidized to obtain sandstone wettability and subsequently it is anodically bonded to a flat glass instead of fusion in the traditional glass-etched micromodel. The Appendix reports on the methodology used for the fabrication of a 2-D glass etched micromodel.

The majority of investigations so far was limited to replica of porous media. To our knowledge a systematic study has not been undertaken for network patterns having fractures along or across the flow direction to study effects of high permeability avenues in the fluid distribution during displacement. As a result, we do not have sufficient knowledge regarding the true mechanisms of drainage and capillary imbibition for oil recovery in fractured reservoirs. Furthermore, the role of fracture in fluid distribution and the relationship between fluid/solid interactions and flow

parameters are ripe subjects for visualization investigations.

2 STEAM INJECTION IN MATRIX-FRACTURE MICROMODELS

Previously, we studied drainage and imbibition processes under fractured systems in isothermal conditions. Steam injection experiments in Hele-Shaw cells were also described to study the flow mechanisms in a geometry resembling a planar fracture. Some aspects of three-phase, two-component flow were demonstrated using a micromodel with dead-end pores. In this report, we complete the investigation by visualization of the flow mechanisms during steam injection in a glass micromodel mimicking the geometry of a matrix-fracture system. We, first, focused on the mechanisms originating from elevated temperature by uniform heating of the model without any fluid injection. Then, the injection of hot water was studied to investigate effects of an elevated temperature in the absence of phase change. Finally, different steam injection was carried out at different capillary numbers. Our observations were analyzed using the previous findings.

2.1 Experiments

The experimental set-up is basically the same as that for the isothermal displacement experiments. In addition, a steam generator consisting of a stainless steel tubing with $\frac{1}{16}$ inch diameter was used. A heater tape with two layers of glass wool were wrapped around the tubing, cold water being pumped into the hot tubing through a check valve using a syringe pump. The syringes for steam generator were of the gas-tight high performance type (Hamilton). The steam temperature was measured and controlled at the entrance of the model by a digital thermocouple temperature controller (Cole-Parmer). The temperature at different parts of the micromodel is measured periodically by a surface probe type T thermocouple. Due to very low steam rate, a high rate of heat loss, consequently a very fast condensation, were experienced. To avoid this, in some experiments we used additional insulation by placing two pieces of glass separated by a rubber spacer on both sides of the micromodel. In some other experiments the model temperature was uniformly raised to decrease the heat losses. The following experiments were undertaken:

1. Heating of a model saturated with crude oil.

2. Hot water displacing crude oil or Dutrex 2621

3. Steam displacing mineral oil or Dutrex 2621.

4. Steam displacing crude oil.

In all experiments, the system was initially saturated with water. Injection of water or oil was done at conditions of secondary imbibition.

2.1.1 Heating of a Model Saturated with Crude Oil

The mechanisms originating strictly from rising the temperature of the model were investigated by the heating of a model saturated with oil, while both outlets were open to the atmosphere. We, first used a California type crude (viscosity 7000 cP at room temperature) in the triangular micromodel. By placing the model on a heater tape, the temperature of the model was slowly increased. Up to 45°C, a small amount of oil production was noticed. Oil expansion was responsible for this small production. At about 50°C, a gaseous phase started to develop (Fig. 1), originating from light components which vaporize. The bubbles nucleated in the micromodel at random places. These bubbles then started to grow towards the fracture (which has lower capillary pressure) (Fig. 2). The process of bubble nucleation and bubble growth have been recently studied by Li [15] in pressure depletion processes and by Satik [24] in boiling processes in porous media. Fig. 3 shows typical ramified shapes of bubble growth and the direction of growth towards the fracture. Fig. 4 shows that most of the crude oil is recovered only by this thermally-induced solution-gas drive at 50°C. Pentane with boiling point of 36.3°C, and hexane with boiling point of 69°C, are examples of light components that may exist and vaporize in crude oil. In order to measure the amount of these light components in our crude sample, we proceeded with a distillation experiment at low temperatures. Only about one percent by volume was collected at 50°C. At that temperature, we also noticed a small amount of non-condensable gas which evolved. In spite of the small amount of light components and dissolved gas, their effects on oil displacement were high due to the sharp contrast in densities between liquid and vapor, which exceeds a ratio of 1000. Thus, 1 percent of pentane in the liquid phase occupies more than 10 pore volumes in gas phase in our model. The associated production was, therefore, significant. In this process, the oil production continued even after gas breakthrough. At this stage, the vaporization involved a large number of snap-off events

in the network (Fig. 5) with lamella created and stabilized by existing natural surfactants in the crude. Due to these snap-off events, much was drained along the roughness of the network.

We should point out that this mechanism was *not* observed during the same experiment involving Dutrex. In the latter case of Dutrex, which is a synthetic oil, no gas phase was observed until the temperature reached around 90°C. At this temperature, full evaporation started, and in a very short time, all the oil was completely recovered.

These experiments show that solution-gas drive process in natural light to medium crudes which contain amounts of light hydrocarboncans can be very important mechanisms during steam displacement.

Figure 1: Bubbles nucleation during uniform heating of crude oil.

2.1.2 Injection of Hot Water

The injection of hot water to displace crude oil or Dutrex, was next carried out in order to study the effect of steam temperature alone without possible phase change or inertia effects. Hot water was injected at 97°C at three different capillary numbers. First, a set of experiments with Bakersfield crude oil in the triangular micromodel were undertaken. The model was initially heated to 40°C to reduce heat loss (but to prevent any vaporization). At the capillary number of 8×10^{-6}, it was

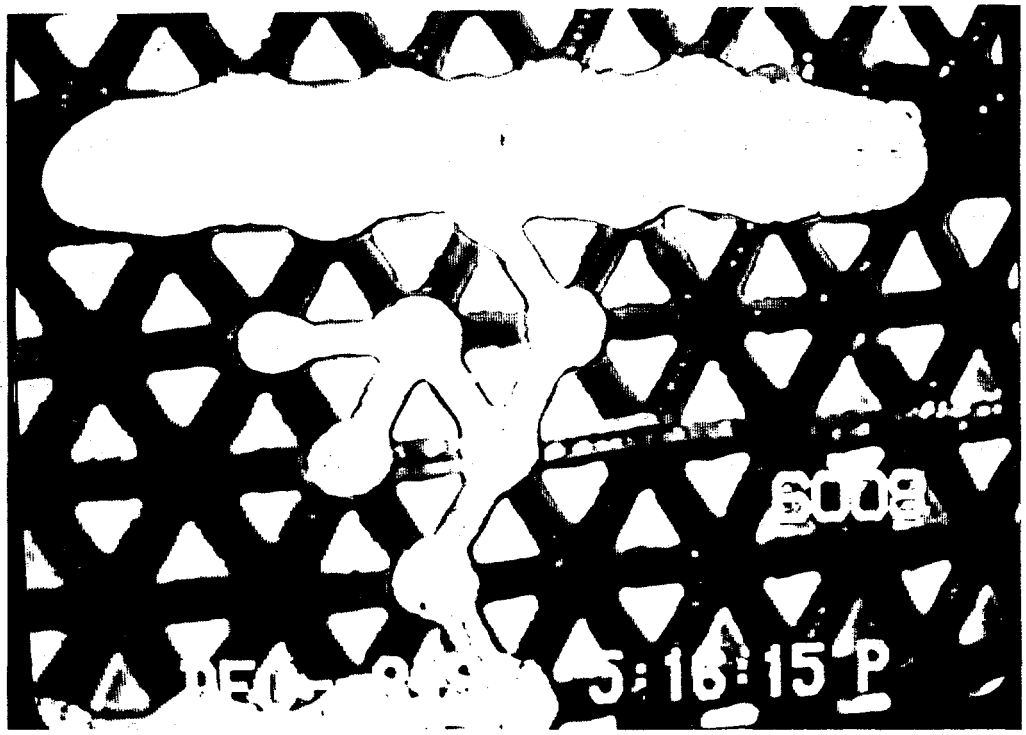

Figure 2: Bubble growth during uniform heating of crude oil.

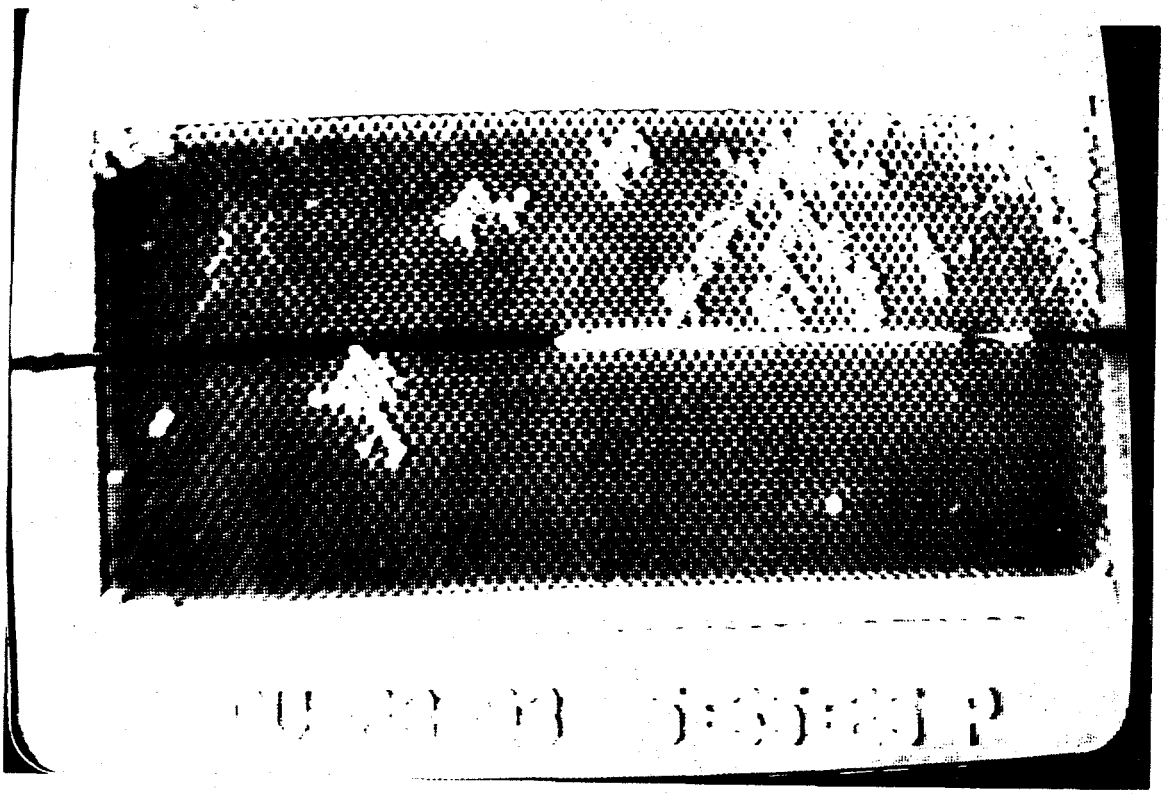

Figure 3: Oil displacement during uniform heating of the model (snapshot 1).

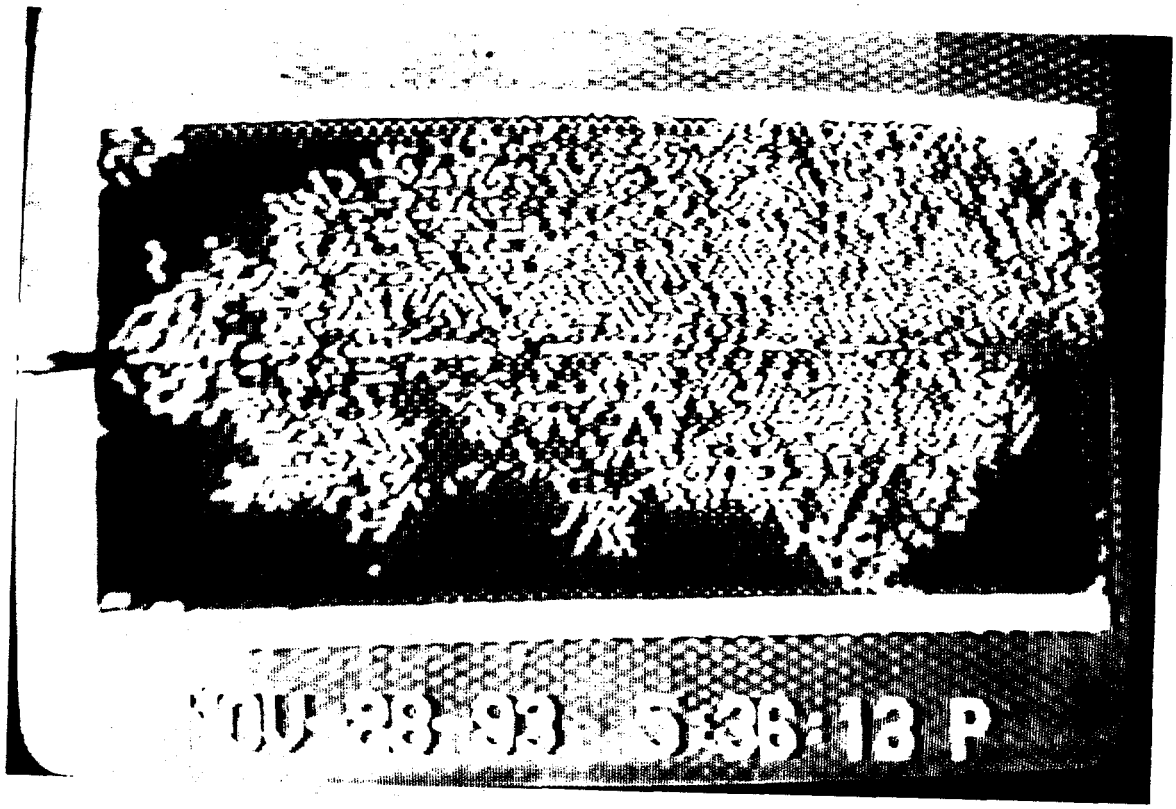

Figure 4: Oil displacement during the heating of the model (snapshot 2).

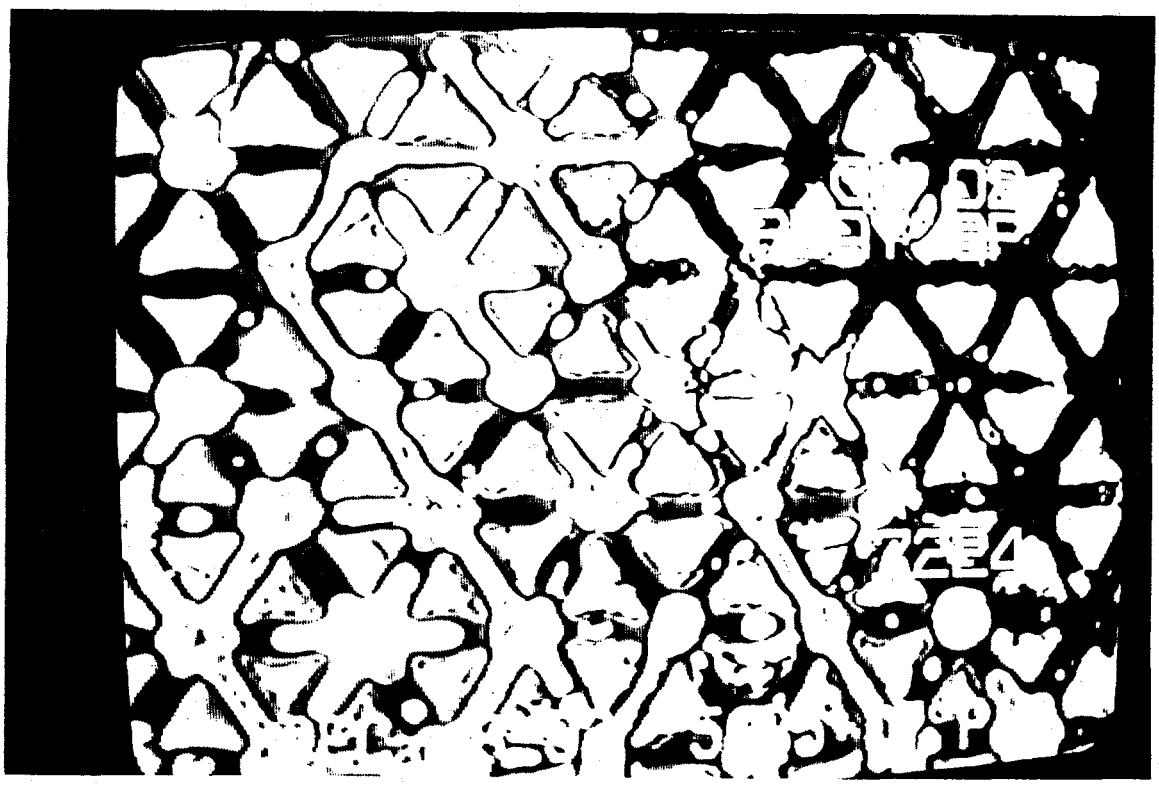

Figure 5: Snap-off after gas breakthrough.

observed that the hot water moved into the fracture first. The fracture was then blocked by a series of relatively stable lamellae. Because of this blockage of the fracture, water is forced to move into the matrix. Fig. 6 shows typical lamellae present in the fracture. When the lamellae created were broken by stretching in the fracture, further water penetration into the matrix was arrested. By the development of new bubbles in the fracture, water started again to invade the matrix. This process continued until all the network were penetrated (Fig. 7). Significantly, no foam was created in the matrix. This is in agreement with the theory of foam flow in heterogeneous media, which offers that foam is created in high permeability zones and forces displacements in low permeability areas. We reiterate that the creation of foam by hot water in the fracture is due to the development of a gas phase in the crude oil at high temperature and the existence of natural surfactants in the crude.

Similar experiments were also carried out with Dutrex as well. Since Dutrex is a synthetic oil, the above components necessary for foam creation are not available; any lamellae created were easily broken.

Subsequent experiments with crude oil continued at the other two capillary numbers, 2×10^{-5} and 4×10^{-5}. Under these conditions, we also observed foam development. However, the lamellae were less stable, because of rate effects which cause lamellae to break more easily than in the case with lower capillary number. It will be seen in the following sections that in the case of steam injection, the high velocity of steam also makes the lamellae to break faster.

Hot water injection was also experimented with the square pattern micromodel. Both crude oil and Dutrex were tested. Here, the fracture was etched twice that in the matrix, and the fracture-to-matrix permeability ratio in this micromodel is much greater than in the triangular. The lamellae resulting from hot water injection were found to be less stable.

2.1.3 Steam Injection

This set of experiments was carried out to examine the application of steam injection, which was the ultimate objective of this dissertation. In this regard, we first carried out preliminary tests with mineral oil and Dutrex, then, a systematic set of experiments with crude oil at different capillary numbers was undertaken.

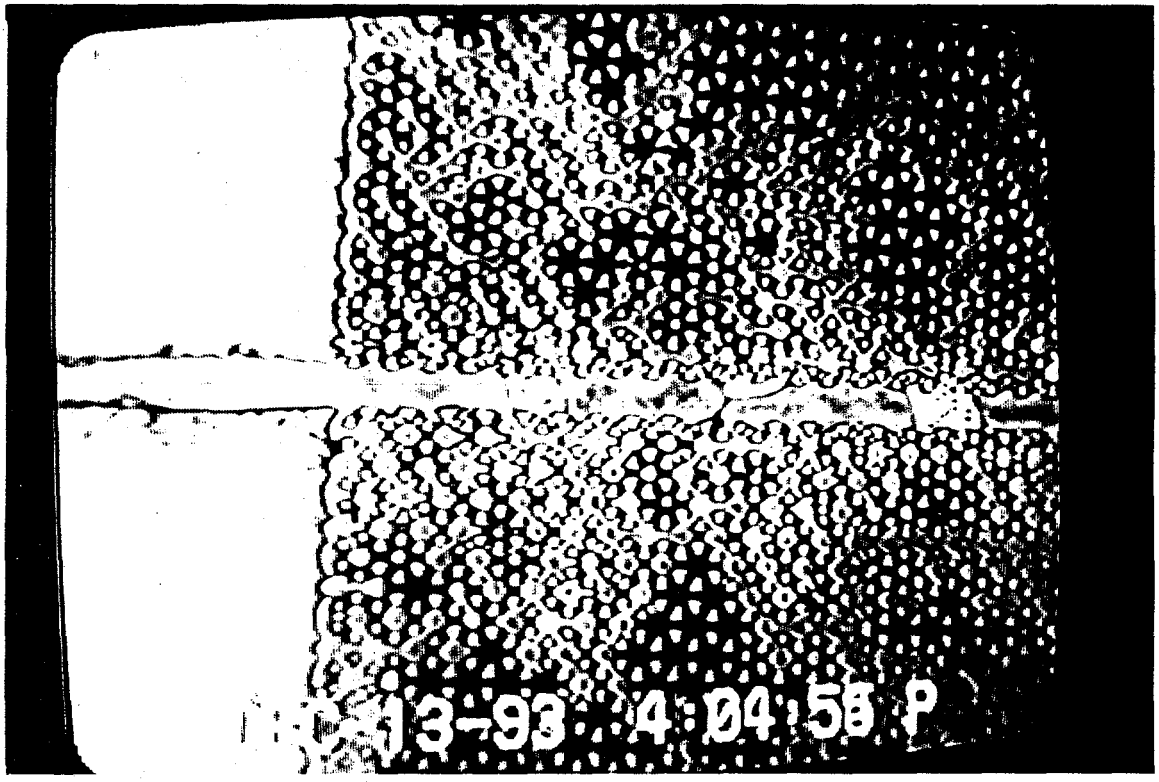

Figure 6: Lamellae in the fracture result from hot water-crude oil displacement.

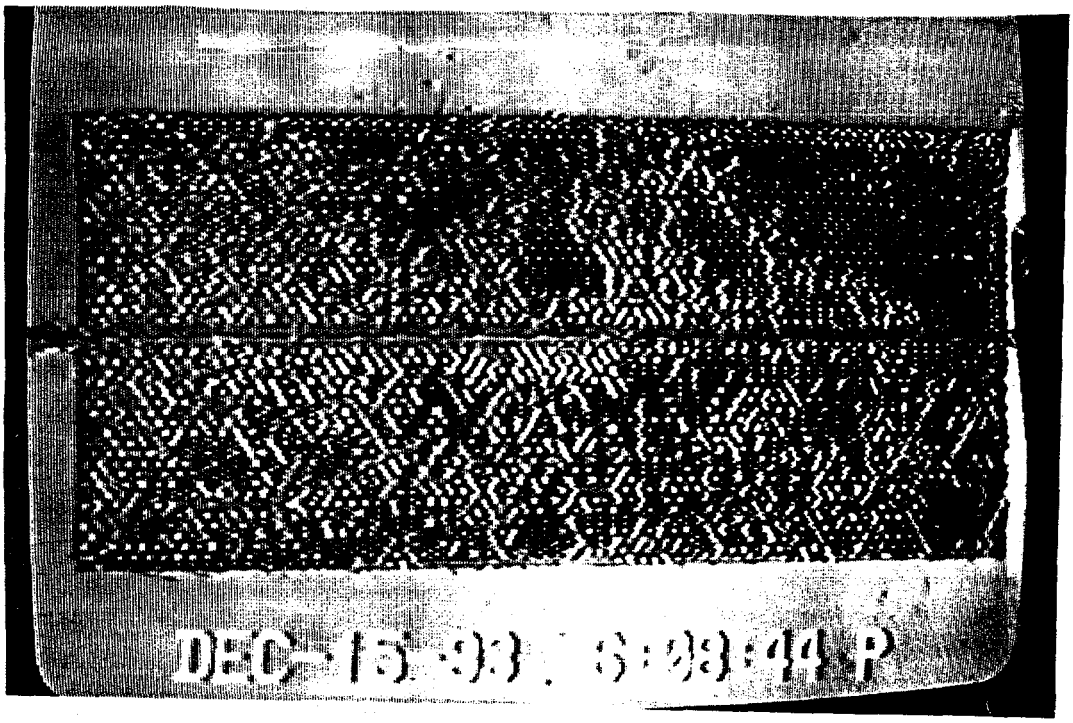

Figure 7: Hot water-crude oil displacement at $Ca = 8 \times 10^{-6}$.

2.1.4 Steam-Mineral Oil Displacement

In steam displacing mineral oil of a viscosity of 100 cP, the triangular pattern micromodel was used. The capillary number based on the equivalent water volumetric rate (0.108 cc/min) was estimated at 8×10^{-6}. The capillary number based on the steam velocity is also the same order of magnitude. Injected steam condensed at the beginning of the injection into the model, the resulting condensed water moving along the fracture first and subsequently penetrating into the matrix. In forced imbibition, the critical capillary number at which the displacement front in the fracture is ahead of the displacement front in the matrix is 5×10^{-6}, which is lower than the capillary number in the experiment. After the area around the inlet of the model became heated, steam started invading the matrix and displaced the remaining trapped oil. Since steam is non-wetting and of a low viscosity, a high velocity is required in order to reach the critical capillary number for the start of invasion of the matrix during drainage. Since we did observe matrix invasion, it can be concluded that the capillary number based on steam velocity is higher than the critical capillary number. The steam front in the fracture, however, is always ahead of that in the matrix (Fig. 8). In areas invaded by steam, due to the traveling of a large volume of steam vapor, and probably lowered interfacial tension at steam temperature, there was virtually no oil trapped. The oil displaced by steam injection moved towards the fracture in the form of an emulsion, while the steam front has the pulsation mechanism similar to what occurred in the Hele-Shaw cell [12], due to the condensation and subsequent restoration. Fig. 9 shows a magnified view of the condensation process in the fracture. After the model became heated, condensation was relatively slow, and the steam front could be visualized for a few seconds. All these observations were also obtained in the experiment with kerosene which has a viscosity of 1.5 cP at room temperature. For both mineral oil and kerosene experiments, no foam generation was observed. The preliminary experiments above show how steam injection in a fractured system involves both drainage and imbibition processes.

2.1.5 Steam-Dutrex Displacement

In this set of experiments, we concentrate on the pore level mechanisms of steam displacement and the role of different fracture configurations. The micromodel in this experiment consisted of a square network adjacent to which are two fractures, one at the inlet perpendicular to flow direction, and another along the flow direction. Steam was introduced through the entire inlet by three paths

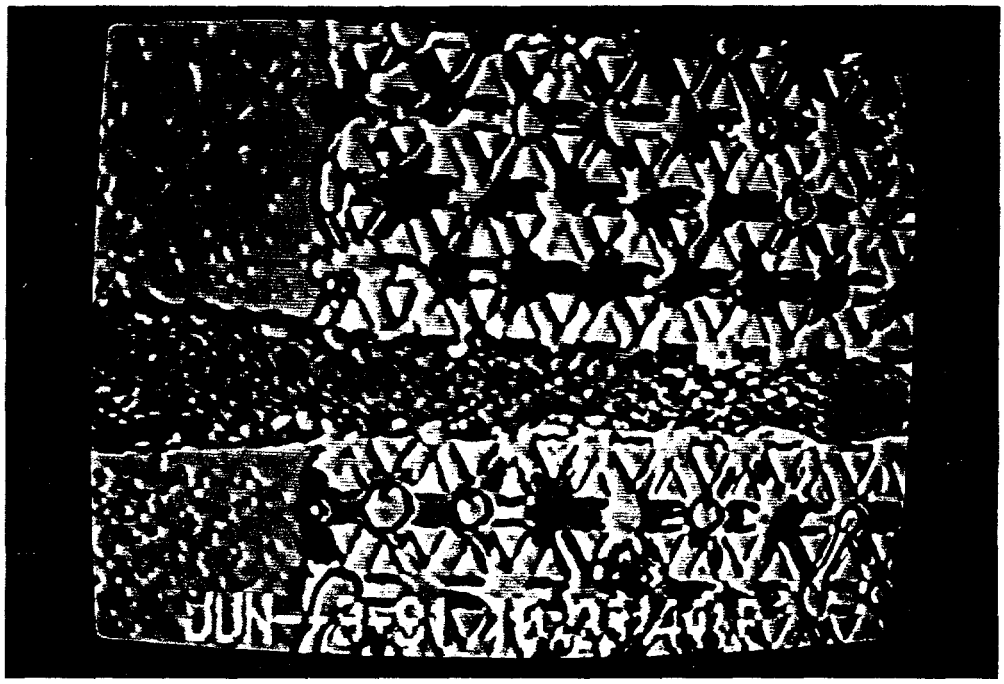

Figure 8: Steam displacing mineral oil

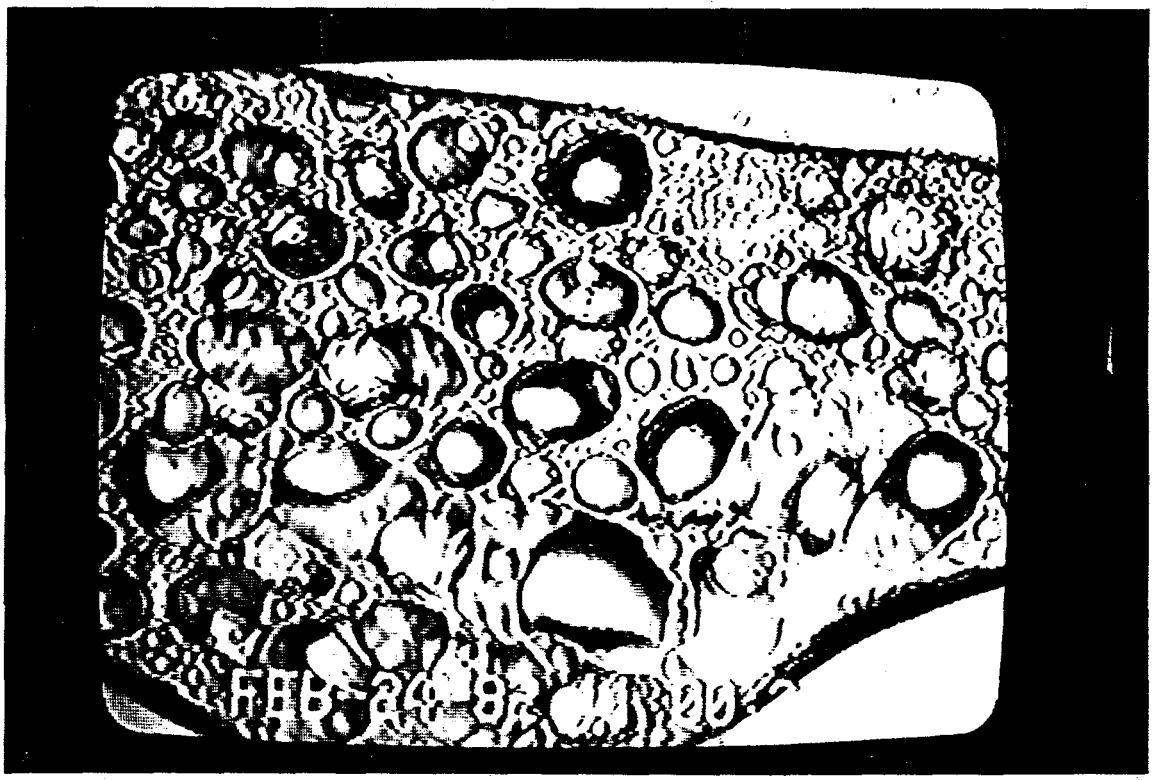

Figure 9: Close-up of steam in the fracture.

etched in the micromodel from the injection port. The model was prewet. The capillary number based on equivalent water velocity was 8×10^{-6}. Due to the two-dimensionality of the model, there was a lack of communication between the condensed displacing water and the water film previously residing at the walls and corners of the network. Thus, condensed water first invaded the oil by meniscus movement only (Fig. 10). Then, it came into contact with preexisting water at the wall and displaced the oil. Fig. 11 shows water droplets in oil, which originated from the first contact of steam with the oil in fracture. Black areas in Fig. 12 show emulsions along the sides of the fracture.

Figures 13 and 14 show two snapshots of the experiment of steam displacing Dutrex. At the start of the experiment, steam moved through both fractures (Fig. 13). Later, steam penetrated into matrix network mostly from the inlet fracture rather than from the fracture along the flow direction (Fig. 14). This appeared to occur because of the high pressure drop near the inlet.

Fig. 15 shows an experiment of steam displacing Dutrex when the model was preheated to 50° C. In this experiment, condensation of steam is much slower and the steam front is much more stable (at 50° C, the viscosity of Dutrex is decreased substantially and the resulting pressure drop is lowered). Additionally, less heat loss due to a higher surrounding temperature produced less condensation.

2.1.6 Steam-Crude Oil Displacement

After these preliminary experiments, a parametric study of a steam-crude oil displacement at three different capillary numbers was undertaken. In this set of experiments, the micromodel with the triangular network was used. We employed a heavy crude sample from California with viscosity of about 7000 cP at room temperature. Steam was injected at three different rates with corresponding capillary numbers of 8×10^{-6}, 2×10^{-5}, and 4×10^{-5}. The capillary numbers were calculated based on an equivalent cold water velocity. In order to be able to compare steam-flooding with water-flooding under similar conditions, we also injected cold water at the same capillary numbers as above. In all experiments either steam or water injection, the crude was initially maintained at the temperature of 40°C. This preheating was necessary to decrease heat losses during steam injection. (Higher temperatures were not tried since at temperatures around 45°C, a gaseous phase from the light components of crude or dissolved gas started to develop).

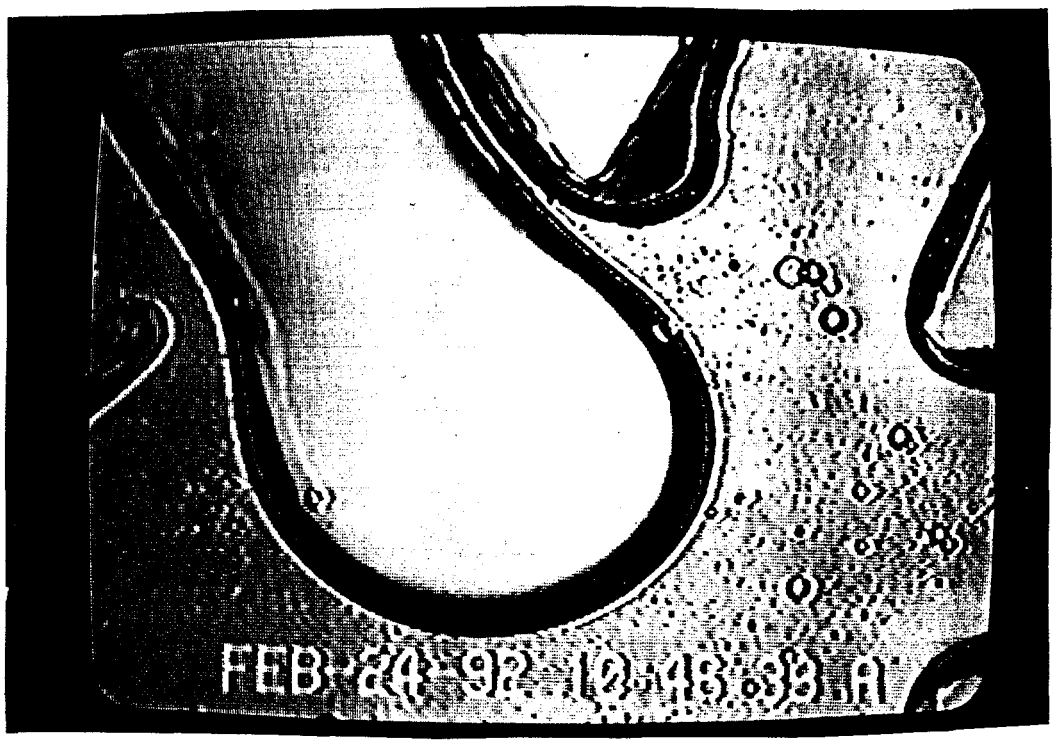

Figure 10: Close-up of condensed water invading oil by meniscus displacement.

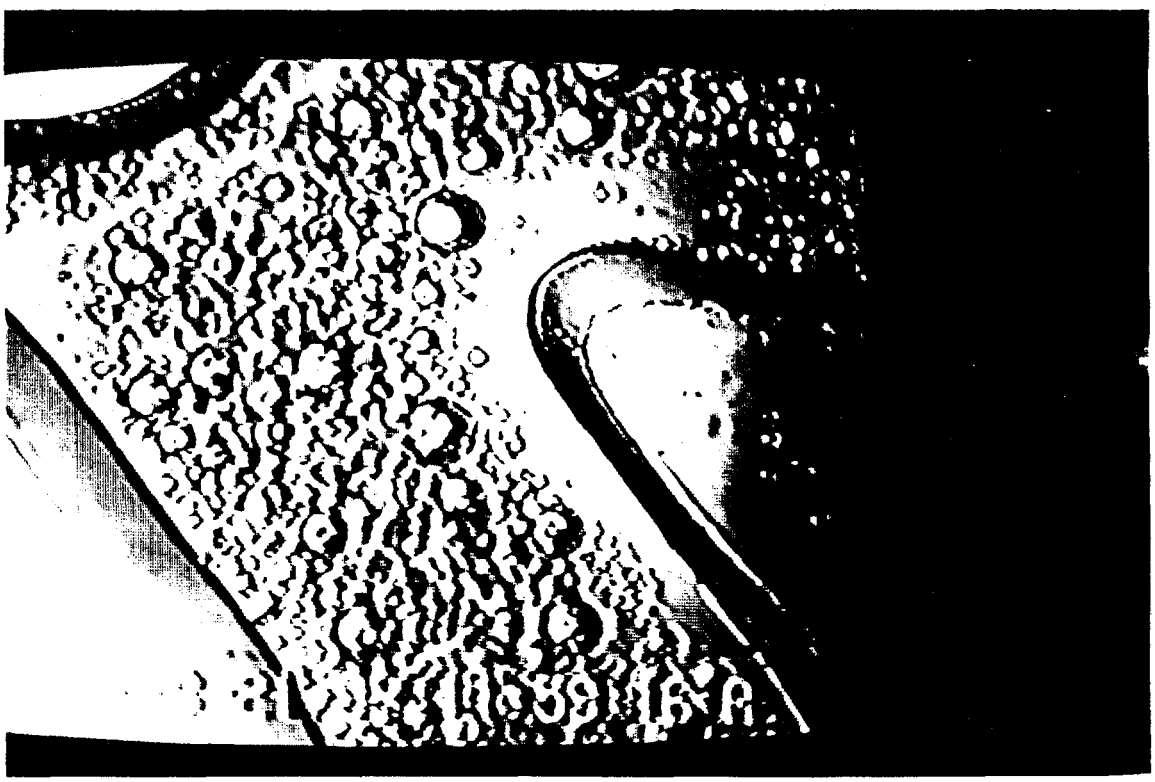

Figure 11: Close-up of water-in-oil emulsion.

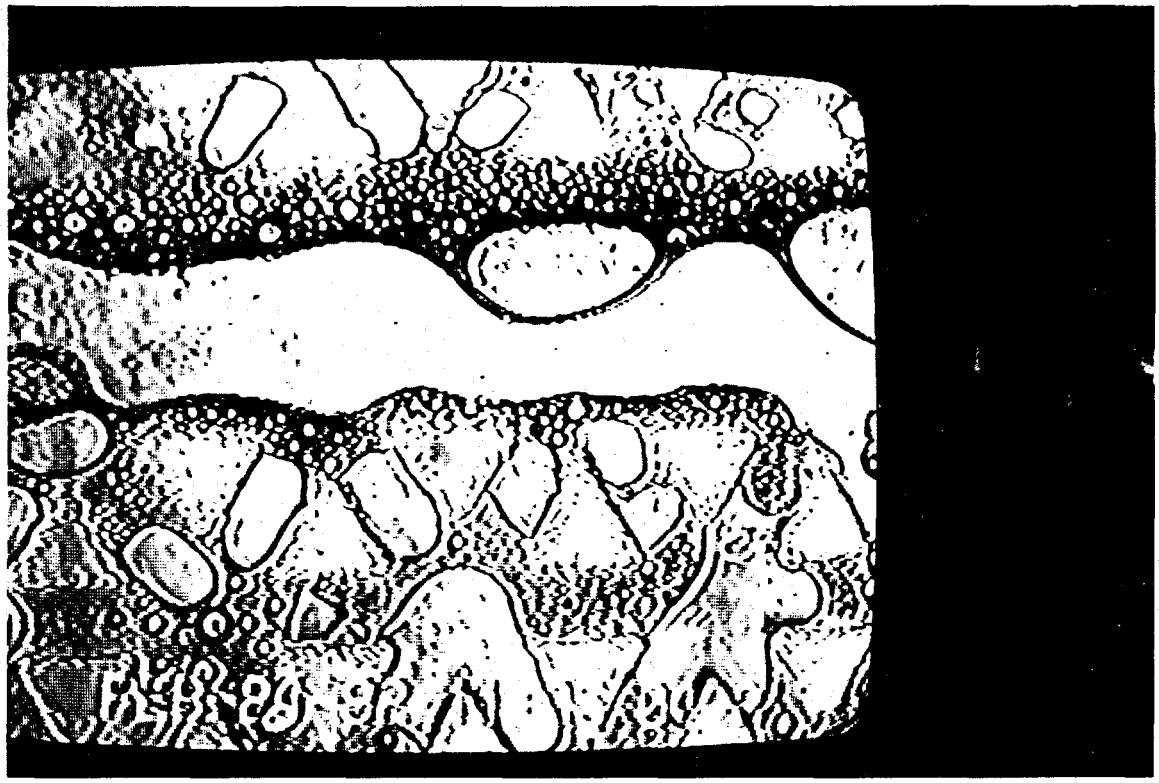

Figure 12: Emulsion along the sides of the fracture.

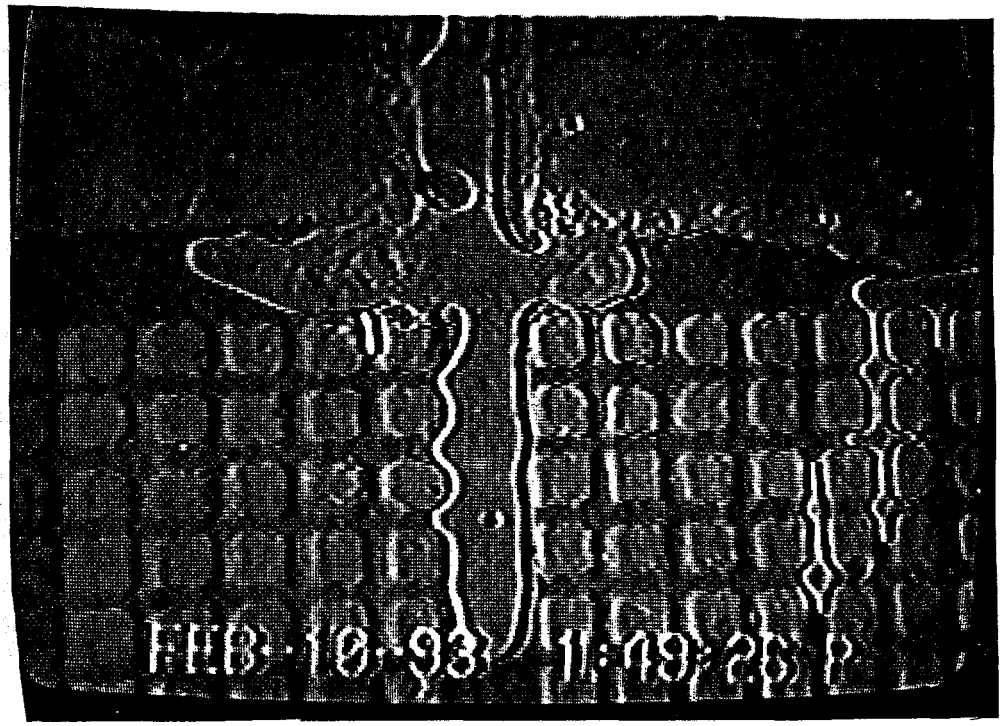

Figure 13: Steam displacing Dutrex (snapshot 1).

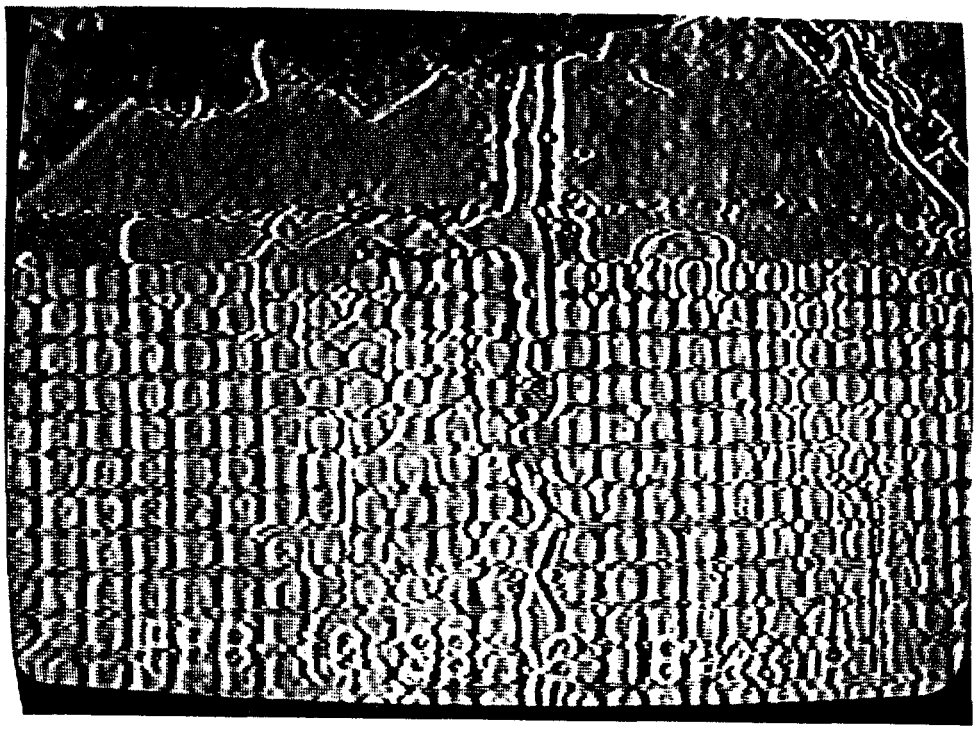

Figure 14: Steam displacing Dutrex (snapshot 2).

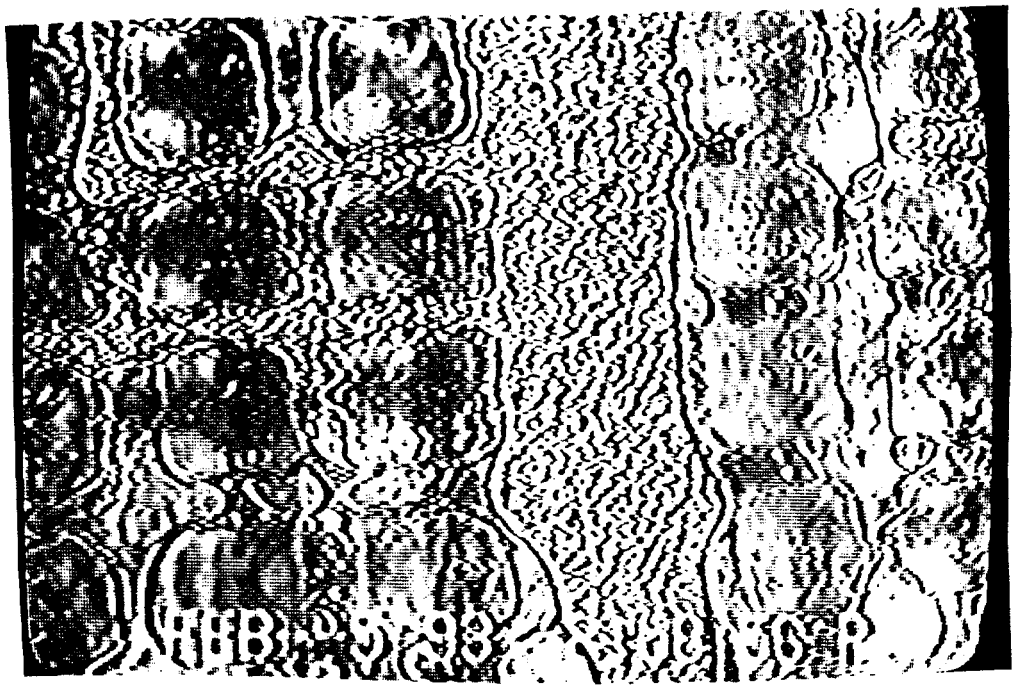

Figure 15: Steam displacing Dutrex (preheating at 50° C).

Steam injection at $Ca = 8 \times 10^{-6}$: The first steam injection experiments started with the rate of 0.108 cc/min of equivalent cold water which corresponds to $Ca = 8 \times 10^{-6}$. The model was preheated at 40°C. At this temperature bubbles did not nucleate. Since the steam rate was low, and due to the initial presence of oil in the fracture, the steam condensed right at the inlet. The condensed water moved first through the fracture, with only a few pores penetrated in the matrix. We reason that this occurred because the rate of water is higher than the critical rate for imbibition, in which the displacement front in the fracture is ahead of the displacement front in the matrix. Also, the corresponding capillary number is barely higher than the critical capillary number for drainage. A drainage process may be applicable if we assume that the water is non-wetting due to the lack of communication with the connate water in a 2-D model when a heavy oil is present. In either case the capillary number does not suffice for a considerable penetration in the matrix. After steam injection continued, additional condensed water penetrated in the matrix (Fig. 16). The reason for this is that at the steam temperature, gas bubbles evolved and temporarily blocked the fracture, resulting into a high pressure drop which led to a displacement towards the matrix. Fig. 17 shows snapshot of steam displacement. It is important to notice that steam moves through the fracture, with only a few pores invaded in the matrix. Fig. 18 shows a close-up of steam in the fracture. In spite of the fact that all oil around the fracture was completely displaced and there was not substantial pressure drop due to the presence of oil, steam moves preferentially through the fracture. We explain this by noting that steam is the non-wetting phase and at capillary number values below the critical for invasion of matrix in drainage, no penetration is expected to occur. Fig. 19 is another snapshot of the experiment in which most of the oil is displaced, while the steam front in the fracture has reached to about half of the model. In another experiment, cold water was injected to displace oil at the same conditions. Cold water similar to the condensed water did enter the fracture at the beginning of steam injection. After some time, a small area near the inlet was also penetrated with water (Fig. 20). By comparison of water-flooding and steam-flooding experiments, we can measure the efficiency of steam displacement in fracture systems. Thermally induced solution gas drive and viscosity reduction are the main mechanisms for the increased efficiency.

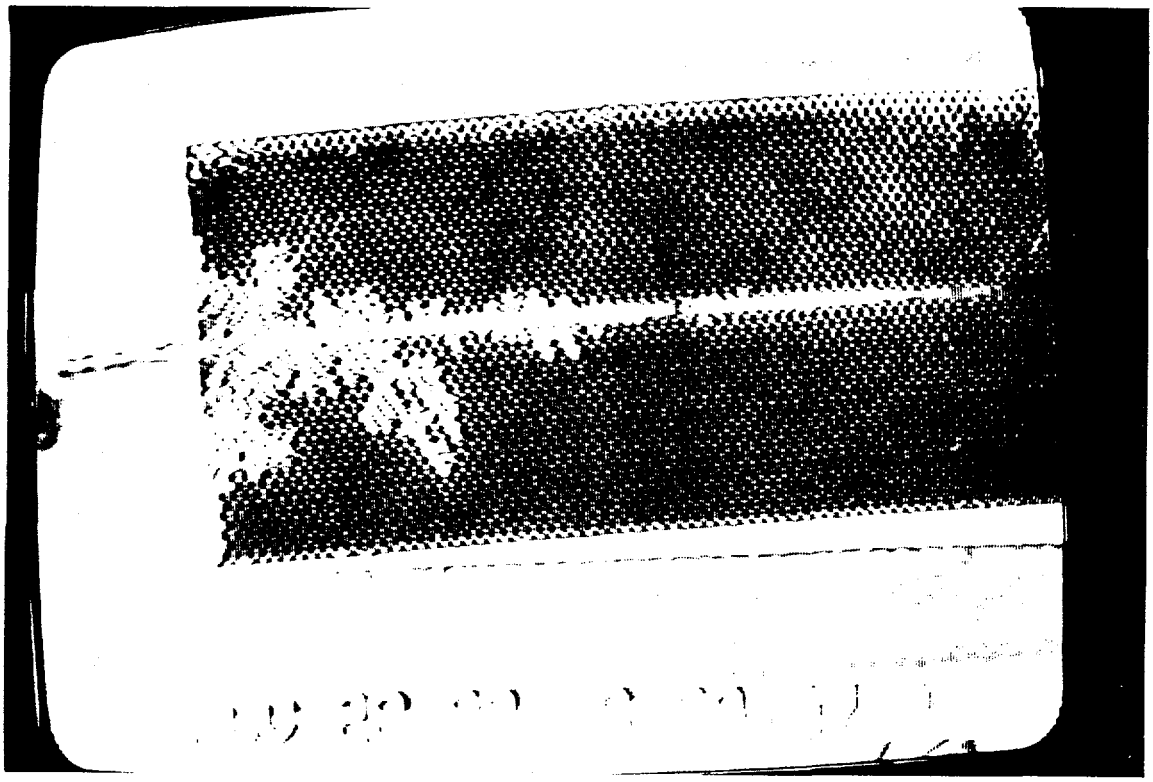

Figure 16: Steam displacing crude oil at $Ca = 8 \times 10^{-6}$ (snapshot 1).

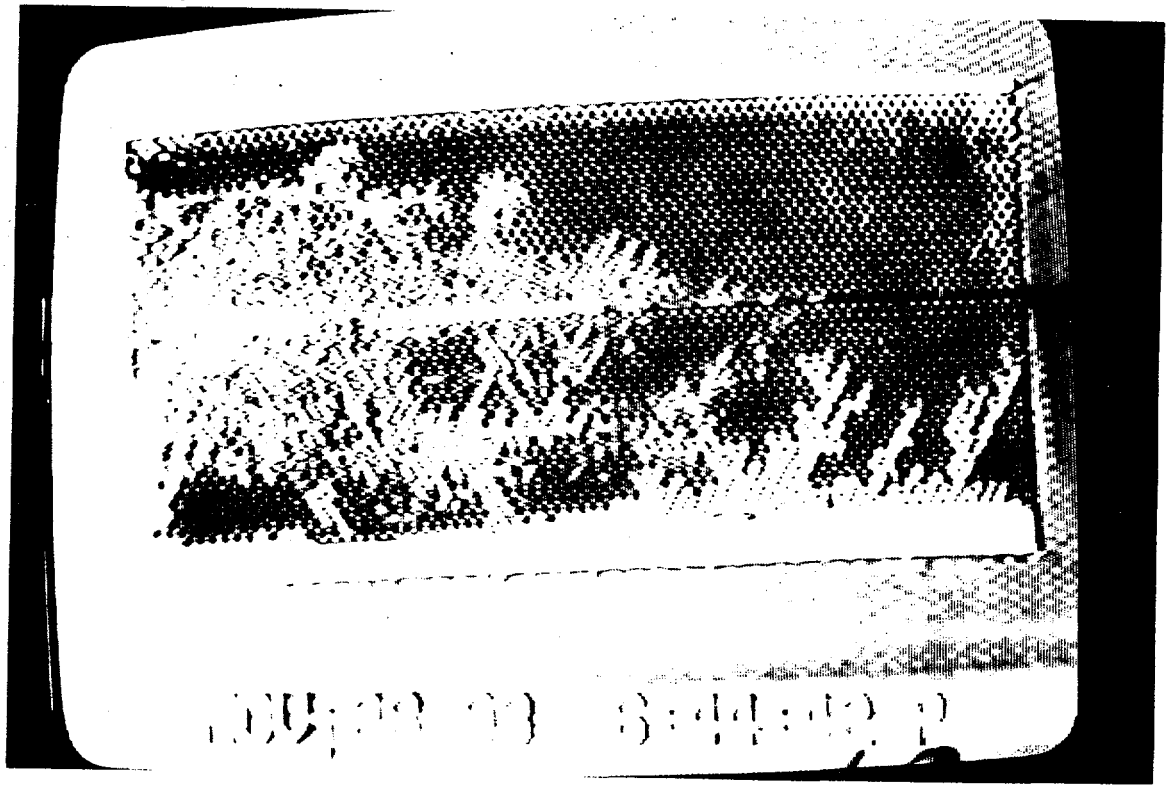

Figure 17: Steam displacing crude oil at $Ca = 8 \times 10^{-6}$ (snapshot 2).

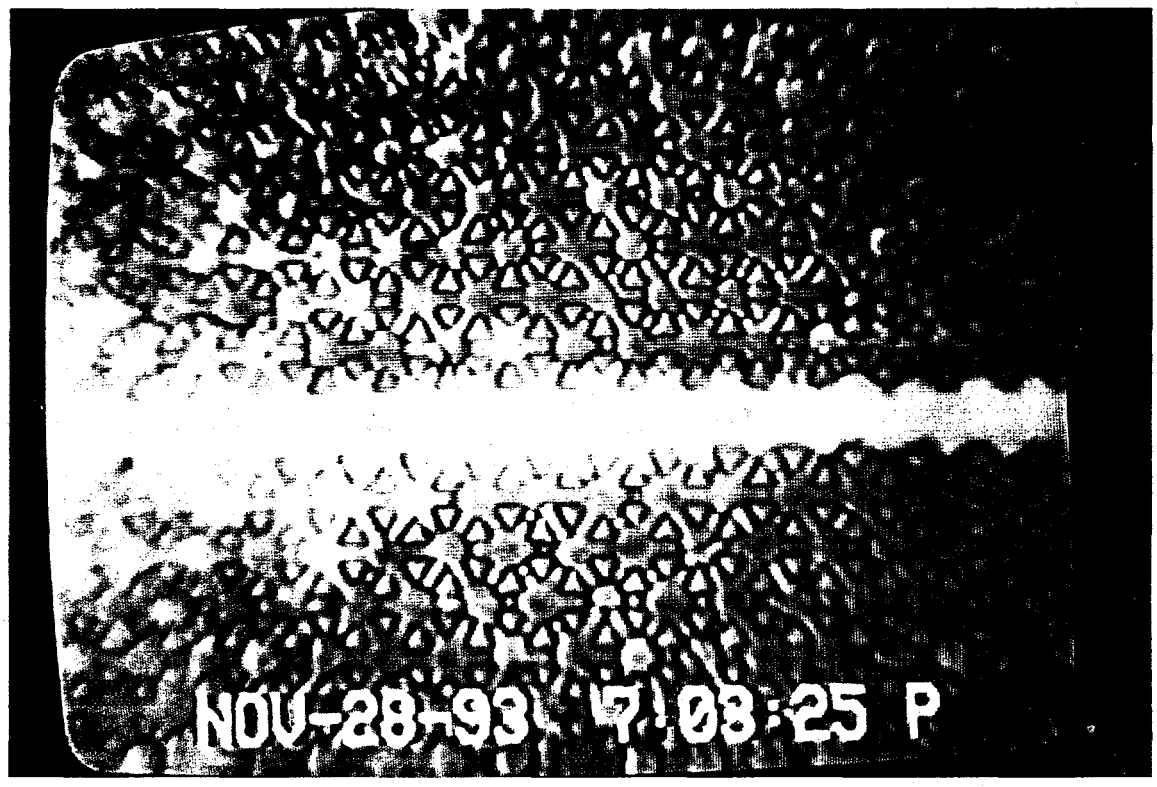

Figure 18: Close-up of steam in fracture during steam-crude oil displacement.

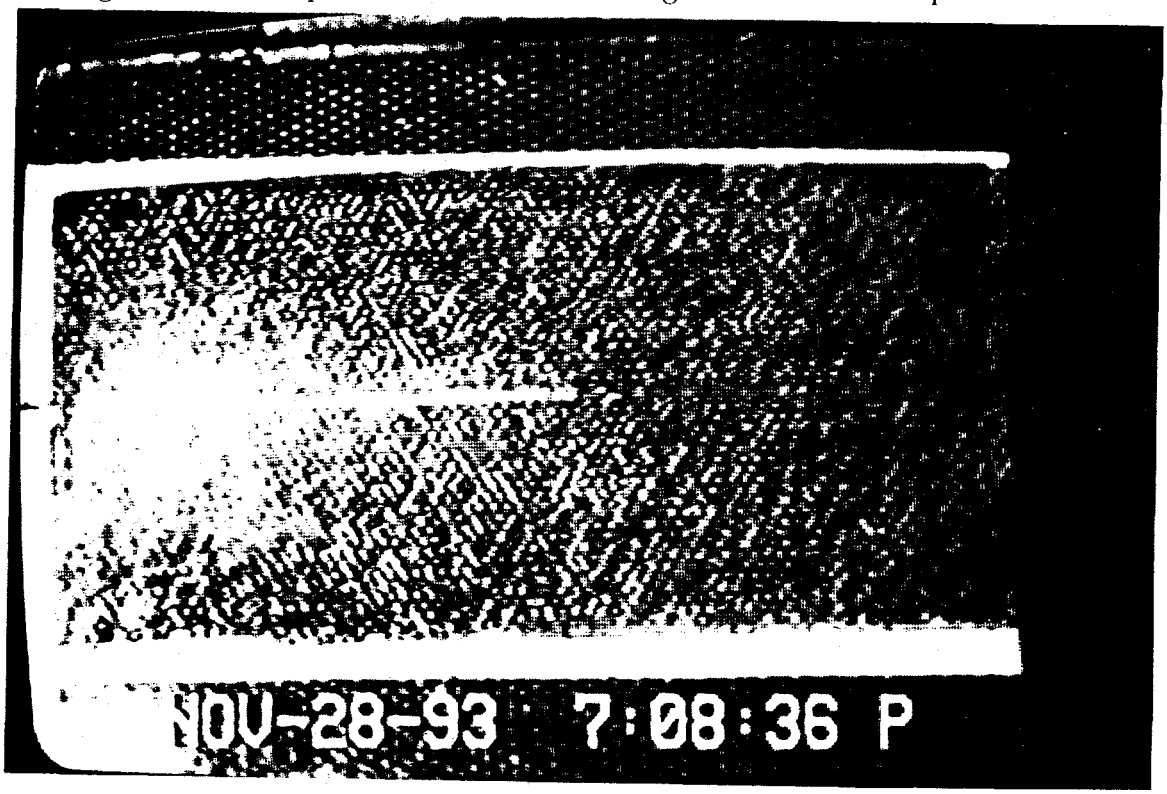

Figure 19: Steam displacing crude oil at $Ca = 8 \times 10^{-6}$ (snapshot 3).

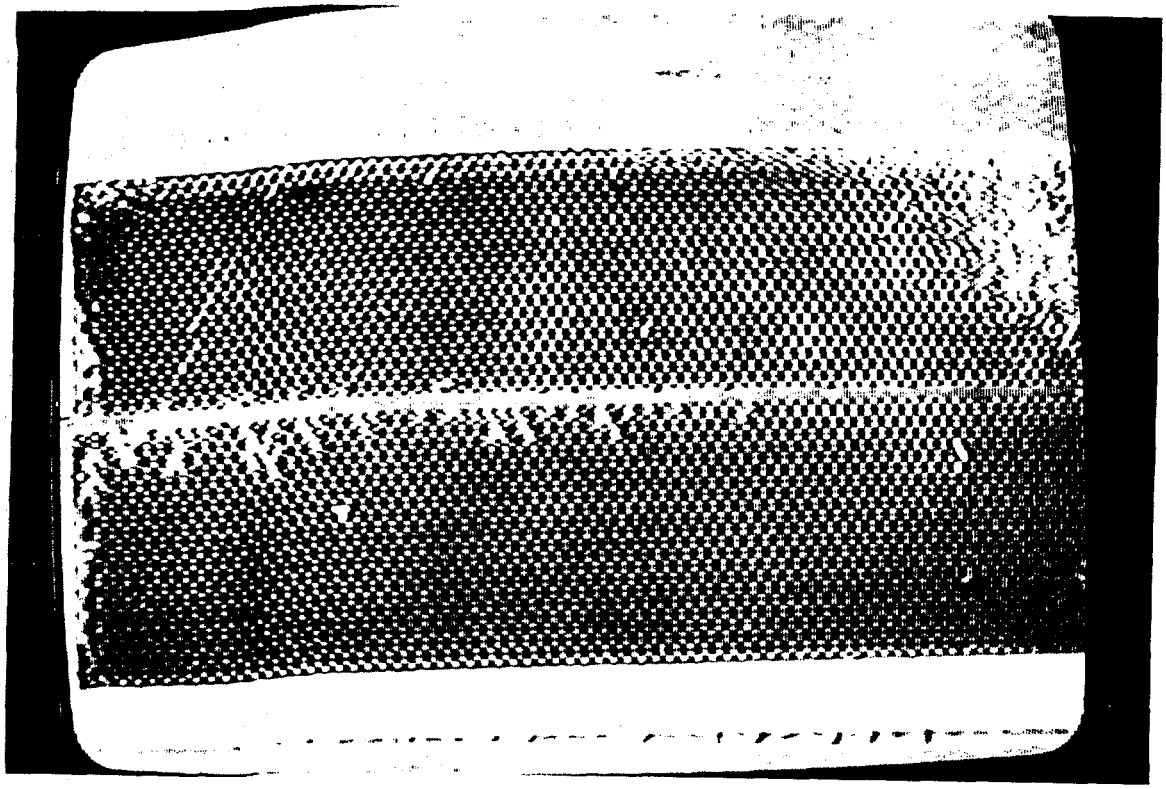

Figure 20: Cold water displacing crude oil at $Ca = 8 \times 10^{-6}$.

Steam injection at $Ca = 2 \times 10^{-5}$: Steam injection experiments were then conducted at the capillary number $Ca = 2 \times 10^{-5}$. The beginning of this experiment is similar to the previous. Condensed water enters the model and first displaces all oil in the fracture (Fig. 21). This is due to the fact that the corresponding capillary number is higher than the critical for either imbibition or drainage. After some steam injection, steam did penetrate the matrix. Fig. 22 shows that steam enters the matrix indicating that the critical capillary number condition is met. The steam fronts in the fracture and matrix are shown in Fig. 23, where the steam in the fracture is ahead of that in the matrix. We note that in those areas displaced by steam, there is no residual oil. Here, similar to the previous, a cold-water injection at the same conditions was also carried out. Now, a viscous finger was created in the matrix in addition to the displacement in fracture (Fig. 24). Nonetheless, the difference between steam and cold water displacement efficiency is clear.

Steam injection at $Ca = 4 \times 10^{-5}$: Finally in the last experiment, the capillary number $Ca = 4 \times 10^{-5}$ was tested both for steam injection and cold water experiments. Figures 25 and 26 show two snapshots of steam injection, while Fig. 27 shows the cold water experiment. In Fig. 25, an early finger in the matrix is observed, as a result of the condensed water. Similar fingers were

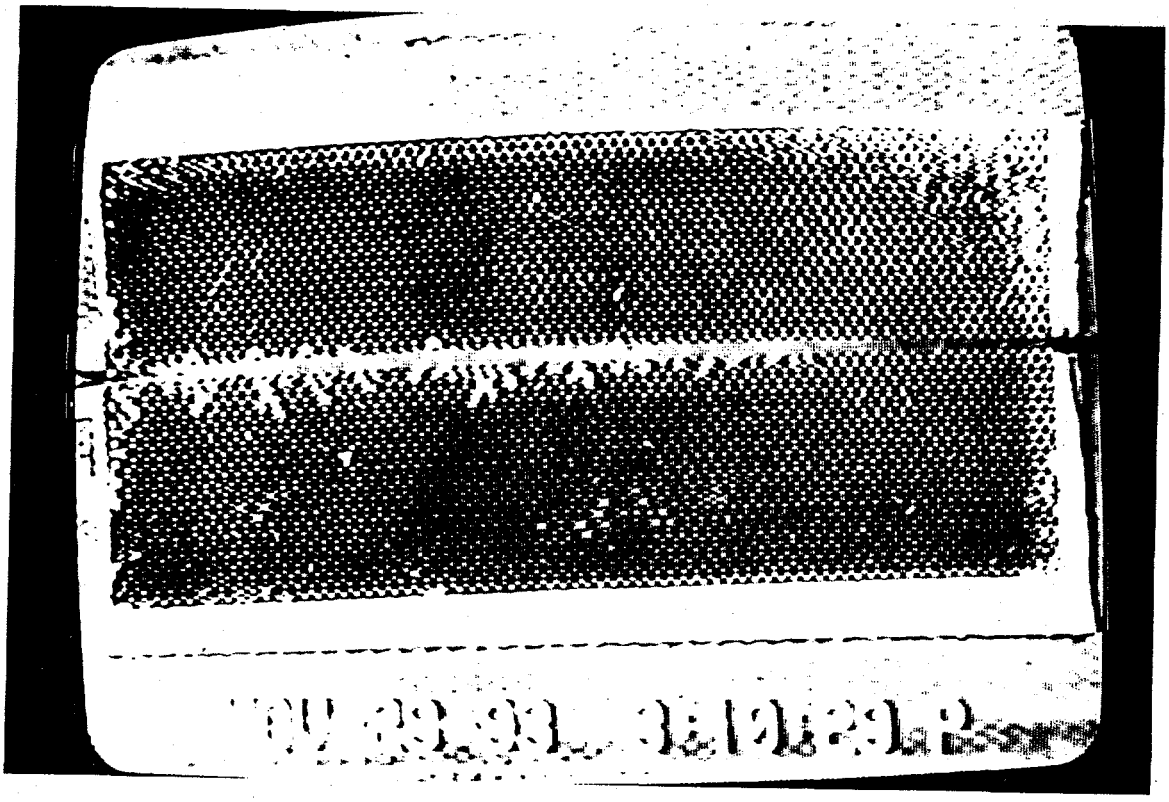

Figure 21: Steam displacing crude oil at $Ca = 2 \times 10^{-5}$ (snapshot 1).

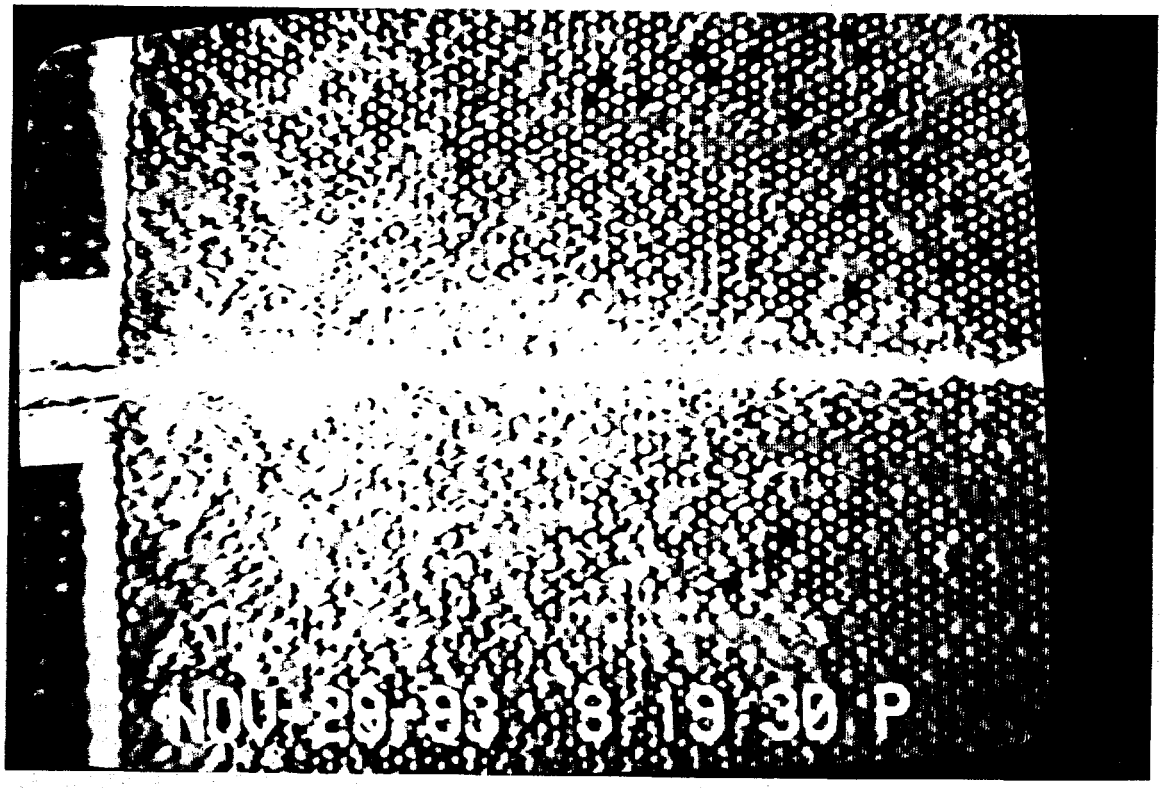

Figure 22: Steam displacing crude oil at $Ca = 2 \times 10^{-5}$ (snapshot 2).

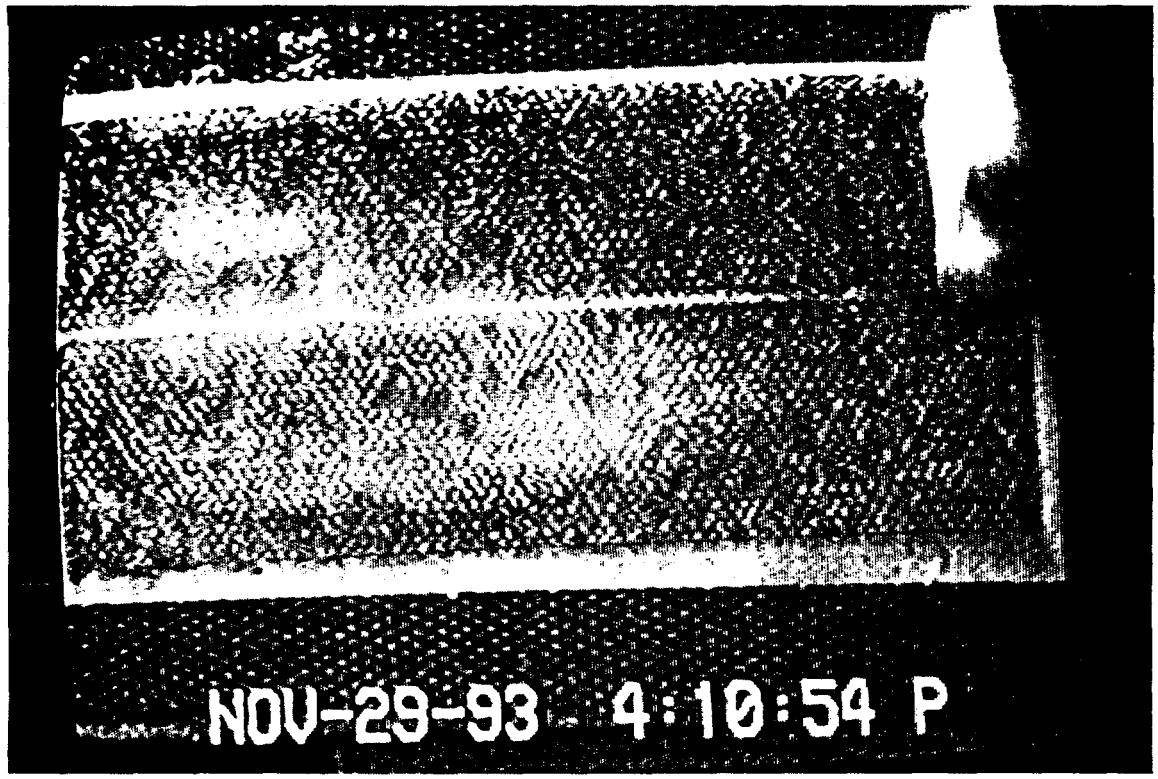

Figure 23: Steam displacing crude oil at $Ca = 2 \times 10^{-5}$ (snapshot 3).

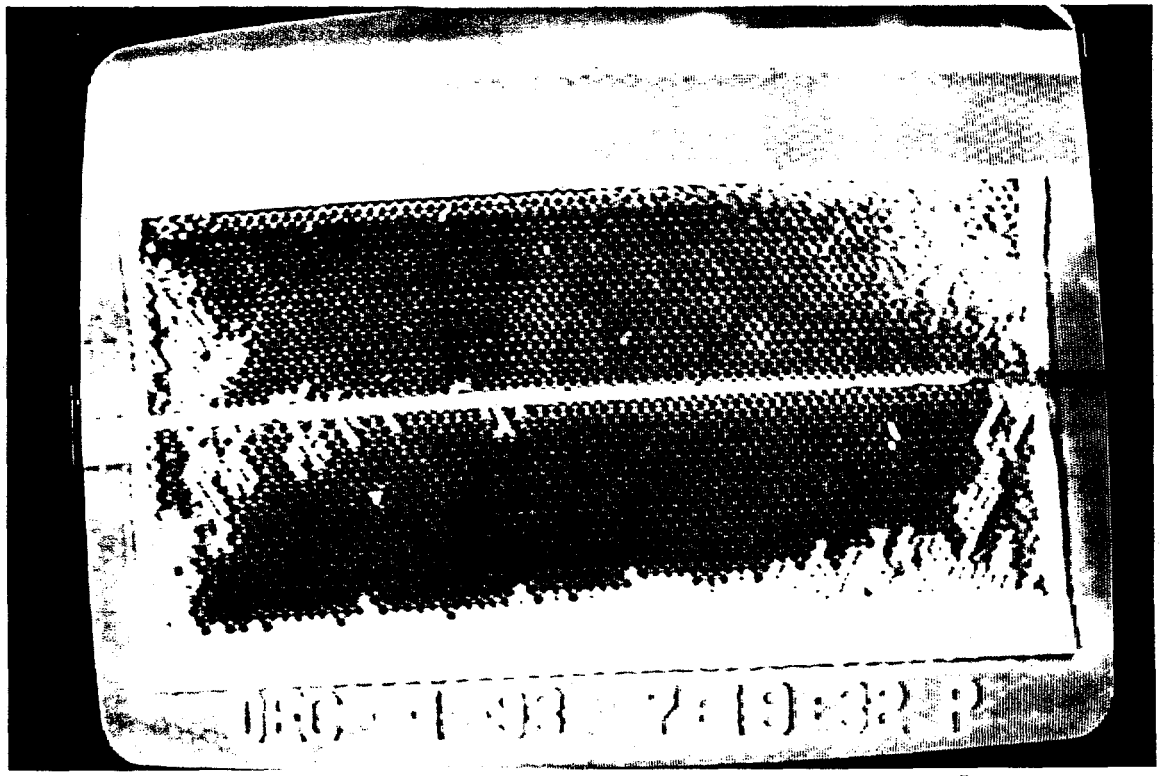

Figure 24: Cold water displacing crude oil at $Ca = 2 \times 10^{-5}$.

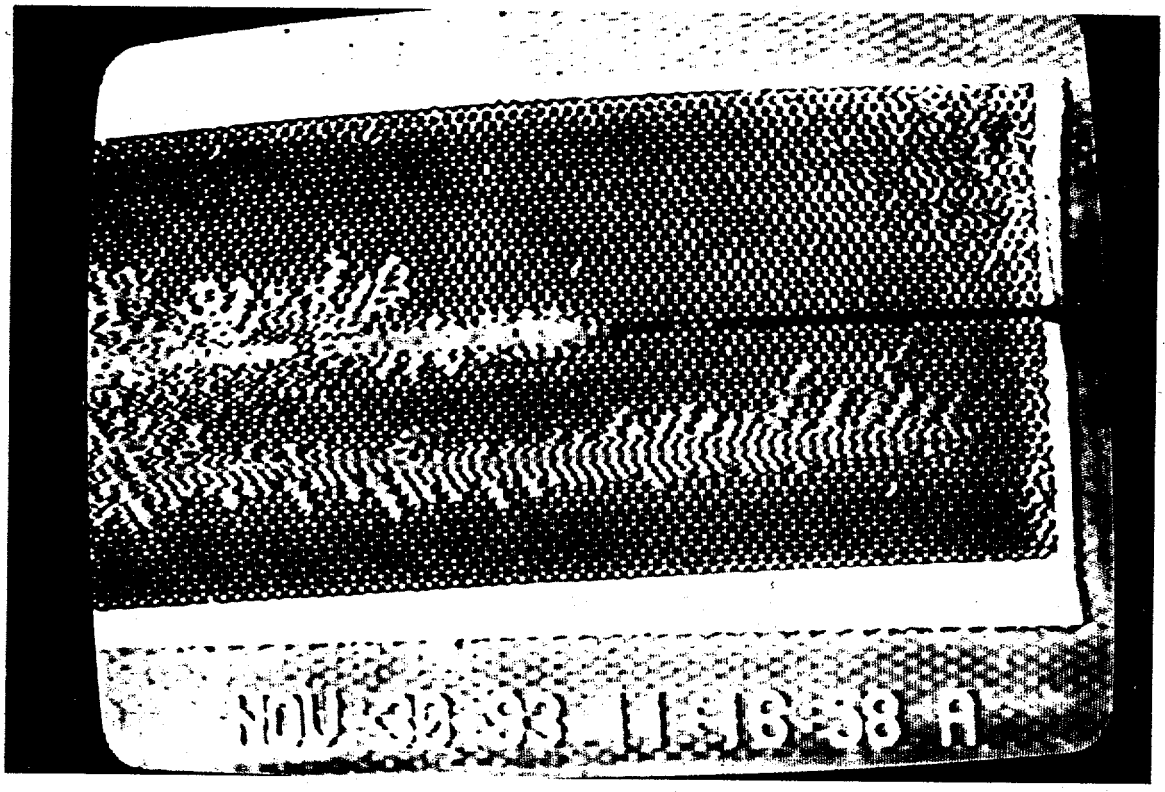

Figure 25: Steam displacing crude oil at $Ca = 4 \times 10^{-5}$ (snapshot 1).

observed in the cold water experiment (Fig. 27). Since the capillary number is relatively high here, we did not detect any imbibition mechanism, but rather a displaced process involving meniscus movement detect. Therefore, Figures 25 and 27 are comparable to the displacement simulated in Fig. 2.15.

3 Conclusions

Pore-level and larger scale visualization of steam and hot water displacement, as well as thermally-induced solution gas drive in a micromodel mimicking a fractured system were carried out. Different oils at different capillary numbers were tested. Also, different configurations of the fracture were examined. In the steam displacement experiments, it was found that the steam enters into the fracture or the matrix depending on the steam rate. If the capillary number exceeds the critical, steam can displace the fluids in the matrix, otherwise it moves into the fracture only. This critical number corresponds to that previously discussed in the isothermal displacement of drainage. Forced imbibition during steam-flooding was also visualized. Whether the condensed water moves preferentially into the fracture or the matrix also depends on the other critical capillary number

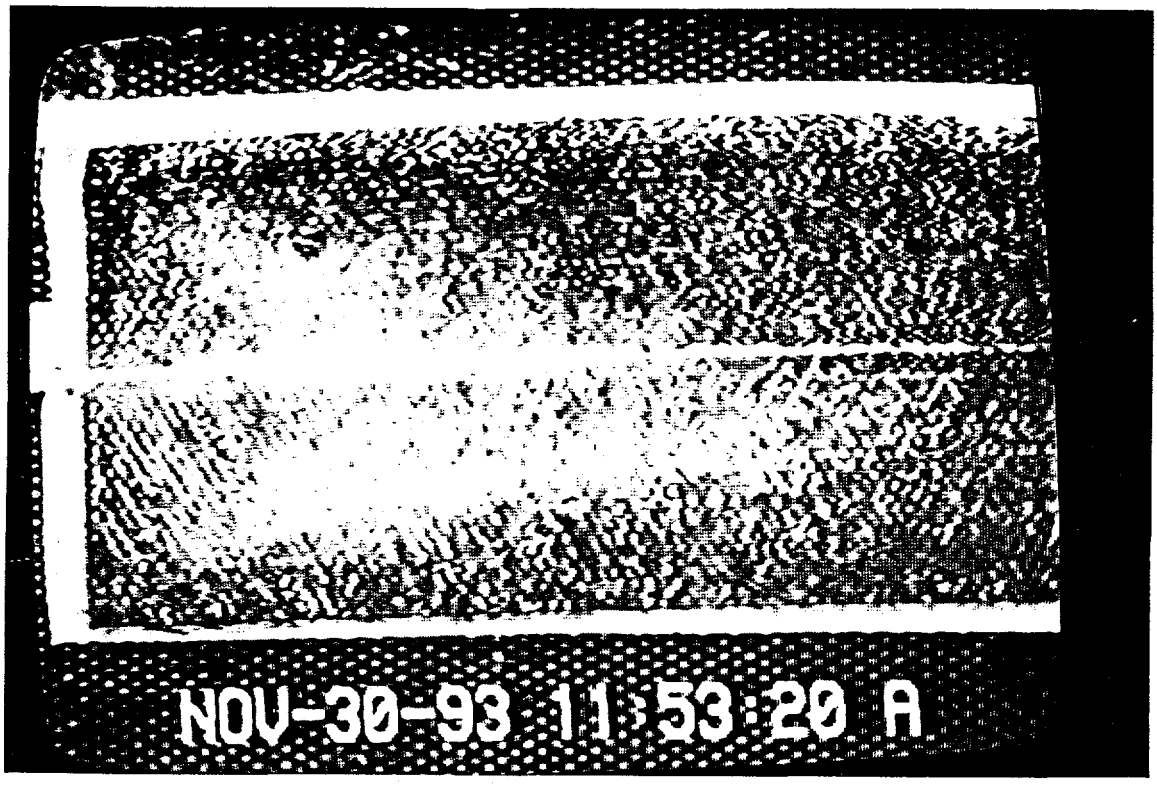

Figure 26: Steam displacing crude oil at $Ca = 4 \times 10^{-5}$ (snapshot 2).

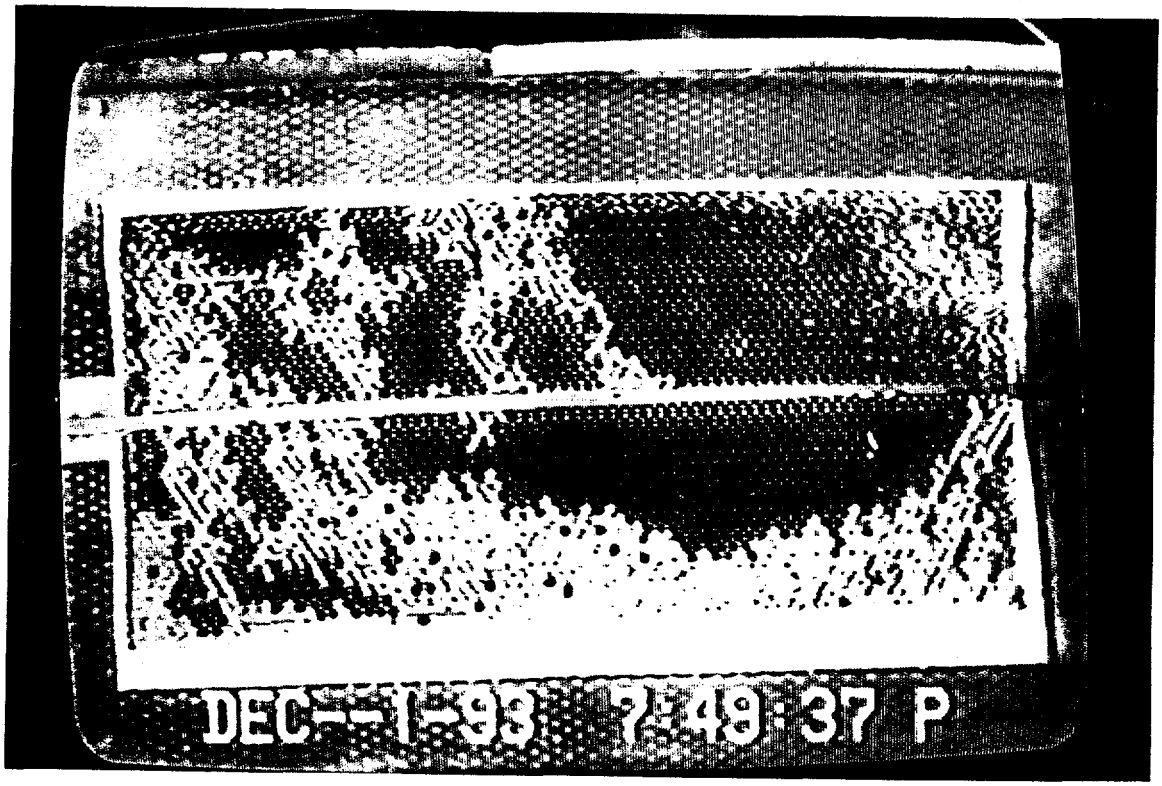

Figure 27: Water displacing crude oil at $Ca = 4 \times 10^{-5}$.

for imbibition, which was found to be a function of the geometric properties of the matrix and the viscosity ratio. At the pore level, it was shown that most of the oil trapped by condensed water can be mobilized and recovered when in contact with steam. A steam pulsation mechanism, due to the condensation and subsequent restoration, was evident. Evaporation of light components existing in crude oil or gas generation may induce a very high efficient gas drive mechanism. Viscosity reduction and oil expansion were observed, as two important effects when steam displaces highly viscous oil. Natural surfactants existing in the crude oil in conjunction with gas generation at high temperatures can lead to the formation of stable lamellae in the fracture and to an improved displacement in the matrix. In general, we found that steam displacement in fractured systems can be an efficient EOR process.

References

[1] T.C. Boberg. *Thermal Methods of Oil Recovery.* John Wiley & Sons, Inc., New York, 1988.

[2] C. E. Brown and E.L. Neustadter. *J. Can. Pet. Technology*, 19:100, 1980.

[3] J. S. Buckley. In *Interfacial Phenomena in Petroleum Recovery*, editor: N.R. Morrow, Marcel Dekker Inc., New York, 1990.

[4] K. T. Chambers and C. J. Radke. In *Interfacial Phenomena in Petroleum Recovery*, editor: N.R. Morrow, Marcel Dekker Inc., New York, 1990.

[5] W.H. Chen, M.L. Wasserman, and R.E. Fitzmorris. Paper SPE 16008 presented at the 1986 SPE Symposium on Reservoir Simulation, San Antonio, February 1-4, 1987.

[6] A. Danesh, J.M. Peden, D. Krinis, and G.D. Henderson. Paper SPE 16956 presented at the 62nd SPE Annual Meeting, Dallas, TX, 1987.

[7] J.A. Davis and S.C. Jones. *J. Pet. Tech.*, 20:1415, 1968.

[8] K.D. Dreher, D.E. Kenyon, and F.D. Iwere. Paper presented at the SPE/DOE fifth symposium on enhanced oil recovery, Tulsa, Oklahama, 1986.

[9] F.A.L. Dullien. *Fluid Transport and Pore Structure.* Academic Press, New York, 1979.

[10] J.W. Hornbrook, L.M. Castanier, and P.A. Pettit. Paper presented at SPE the 66th Annual Technical Conference and Exhibition, Dallas, TX, 1991.

[11] T.B. Jensen. Ph.D. Dissertation, Univ. of Wyoming, 1991.

[12] X. Kong, M. Haghighi, and Y.C. Yortsos. *Fuel*, 71:1465, 1992.

[13] B.Y.Q. Lee and T.B.S. Tan. Paper SPE 16009 presented at the 1986 SPE Symposium on Reservoir Simulation, San Antonio, February 1-4, 1987.

[14] R. Lenormand, C. Zarcone, and A. Sarr. *J. Fluid Mech.*, 135:337, 1983.

[15] X. Li and Y.C. Yortsos. Paper SPE 22589 presented at the 66th SPE Annual Meeting, Dallas, TX, Oct. 6-9, 1991.

[16] Y. Li and N.C. Wardlaw. *J. Colloid Interface Sci.*, 109:461, 1986.

[17] C.C. Mattax and J.R. Kyte. *Oil and Gas J.*, 59:115, 1961.

[18] Van P. Meurs. *Trans. AIME*, 210:295, 1959.

[19] P. Persoff, K. Pruess, and L. Myer. Paper presented at 16th Workshop on Geothermal Reservoir Engineering, Stanford University, January 23-25, 1991.

[20] M. Prats. *Thermal Recovery.* SPE, Richardson TX, 1982.

[21] J.C. Reis. Paper presented at the SPE/DOE 7th symposium on enhanced oil recovery, Tulsa, Oklahama, 1990.

[22] B. C. Sahuquet and J. J. Ferrier. *JPT*, page 873, April 1982.

[23] A. M. Saidi. *Reservoir Engineering of Fractured Reservoirs: Fundamental and Practical Aspects.* Total Edition Presse, Paris, 1988.

[24] C. Satik. Ph.D. Dissertation, Univ. of Southern California, 1994.

[25] J. N. M. van Wunnik and K Wit. *SPE Reservoir Engineering*, page 75, Feb. 1992.

[26] B. T. Willman, V. V. Valleroy, G. W. Cornelius, and L. W. Powers. *J. Pet. Tech.*, page 681, 1961.

[27] D. Yang, N.C. Wardlaw, and M. Mekeller. *AOSTRA J. of Research*, 6:123, 1990.

☆U.S. GOVERNMENT PRINTING OFFICE: 1995 - 660-029/20037